ERRATUM

Development 133, 3051 (2006) doi:10.1242/dev.02518

BDNF increases synapse density in dendrites of developing tectal neurons in vivo

Analiza L. Sanchez, Benjamin J. Matthews, Margarita M. Meynard, Bing Hu, Sana Javed and Susana Cohen Cory *Development* **133**, 2477-2486.

An error in the last name of one of the authors was not corrected before this article went to press.

Susana Cohen Cory should have been written as Susana Cohen-Cory.

We apologise to the authors and readers for this mistake.

Development 133, 2477-2486 (2006) doi:10.1242/dev.02409

BDNF increases synapse density in dendrites of developing tectal neurons in vivo

Analiza L. Sanchez*, Benjamin J. Matthews*, Margarita M. Meynard*, Bing Hu*, Sana Javed and Susana Cohen Cory†

Neuronal connections are established through a series of developmental events that involve close communication between pre- and postsynaptic neurons. In the visual system, BDNF modulates the development of neuronal connectivity by influencing presynaptic retinal ganglion cell (RGC) axons. Increasing BDNF levels in the optic tectum of *Xenopus* tadpoles significantly increases both axon arborization and synapse density per axon terminal within a few hours of treatment. Here, we have further explored the mechanisms by which BDNF shapes synaptic connectivity by imaging tectal neurons, the postsynaptic partners of RGCs. Individual neurons were co-labeled with DsRed2 and a GFP-tagged postsynaptic density protein (PSD95-GFP) to visualize dendritic morphology and postsynaptic specializations simultaneously in vivo. Immunoelectron microscopy confirmed that PSD95-GFP predominantly localized to ultrastructurally identified synapses. Time-lapse confocal microscopy of individual, double-labeled neurons revealed a coincident, activity-dependent mechanism of synaptogenesis and axon and dendritic arbor growth, which is differentially modulated by BDNF. Microinjection of BDNF into the optic tectum significantly increased synapse number in tectal neuron dendritic arbors within 24 hours, without significantly influencing arbor morphology. BDNF function-blocking antibodies had opposite effects. The BDNF-elicited increase in synapse number complements the previously observed increase in presynaptic sites on RGC axons. These results, together with the timescale of the response by tectal neurons, suggest that the effects of BDNF on dendritic synaptic connectivity are secondary to its effects on presynaptic RGCs. Thus, BDNF influences synaptic connectivity in multiple ways: it enhances axon arbor complexity expanding the synaptic territory of the axon, while simultaneously coordinating synapse formation and stabilization with individual postsynaptic cells.

KEY WORDS: *Xenopus laevis*, Synapse, Tectal neuron, PSD95-GFP, Branching, In vivo imaging, APV

INTRODUCTION

In the developing central nervous system, functional neuronal circuitry is established as axon terminals arborize, recognize their target neurons and form precise synaptic connections. In vivo imaging studies demonstrate that developing axon terminals are highly dynamic and actively participate in synaptogenesis (Alsina et al., 2001; O'Rourke and Fraser, 1990; Witte et al., 1996). Postsynaptic dendritic arbors are also dynamic, and it is through coordinated interactions between axon and dendritic filopodia that target recognition and synapse formation take place (Cline, 2001; Cohen-Cory, 2002; Dailey and Smith, 1996; Deng and Dunaevsky, 2005; Jontes and Smith, 2000; Niell et al., 2004; Trachtenberg et al., 2002). Proper neuronal connections are thus specified as axons and dendrites make initial contacts and establish synapses that are often transient. Cell-surface adhesion molecules, inductive signals, secreted factors and signaling molecules actively participate in cell-to-cell communication, making neurons receptive to form synapses (Chen and Ghosh, 2005; Ethell and Pasquale, 2005; Waites et al., 2005). Neurotrophins are potent modulators of neuronal morphology, influencing not only axonal arborization (Cohen-Cory and Fraser, 1995; Singh and Miller, 2005) but also dendritic arbor growth (Horch and Katz, 2002; Lom et al., 2002; McAllister, 2000). Neurotrophins can act as target-derived trophic factors to influence presynaptic neurons, and/or as anterograde factors to influence postsynaptic cells (Baquet et al., 2004; Gonzalez et al., 1999; von Bartheld et al., 2001; Zweifel et al., 2005). Retrograde and anterograde signaling by neurotrophins has also been implicated in the modulation of synapse structure and function (Du and Poo, 2004; Elmariah et al., 2004; Rico et al., 2002; Vicario-Abejon et al., 2002; Zhang and Poo, 2002).

In the visual system, BDNF modulates synaptic connectivity by influencing presynaptic specializations in retinal ganglion cell (RGC) axon arbors. Increasing BDNF levels in the optic tectum of live developing *Xenopus* tadpoles significantly increases RGC axon arborization and synaptic density within 4 hours of treatment (Alsina et al., 2001). Conversely, decreasing endogenous BDNF levels destabilizes synapses and axon branches in RGC arbors over a similar timescale (Hu et al., 2005). The rapid impact of BDNF on presynaptic specializations and axon arbor morphology suggests that BDNF modulates synaptic connectivity by acting directly on presynaptic RGCs. It is possible that BDNF influences retinotectal connectivity by also influencing tectal neurons, the postsynaptic partners of RGCs. The expression patterns of BDNF and its receptor TrkB also suggest that BDNF specifically regulates synaptogenesis and the maturation of RGC axons at the target and may also influence tectal neurons directly. BDNF is expressed both in the retina and optic tectum during active retinotectal development. TrkB mRNA is expressed by RGCs and is also expressed in the optic tectum, although at significantly lower levels (Cohen-Cory et al., 1996; Cohen-Cory and Fraser, 1994). Therefore, BDNF may act locally within the optic tectum to influence the development of tectal neurons, either directly or as consequence of its effects on presynaptic RGC axons.

Department of Neurobiology and Behavior, University of California, Irvine, Irvine, CA 92697, USA.

*These authors contributed equally to this work
†Author for correspondence (e-mail: scohenco@uci.edu)

Accepted 18 April 2006

Here, we have used in vivo time-lapse imaging to further explore the mechanisms by which BDNF influences retinotectal synaptic connectivity. Expression of the GFP-tagged postsynaptic density protein PSD-95 together with DsRed2 was used to simultaneously visualize postsynaptic specializations and dendritic arbor morphology in *Xenopus* tectal neurons in vivo. Altering endogenous BDNF levels in the optic tectum by injection of recombinant BDNF or function-blocking antibodies to BDNF demonstrates that BDNF influences tectal neuron synaptic connectivity over a longer timescale than its effects on RGC axon arbors. Surprisingly, manipulations of BDNF levels did not significantly influence dendritic arbor morphology. Time-lapse imaging also revealed a coordinated, dynamic mechanism of synaptogenesis and arbor growth in tectal neuron dendrites that closely resembles that of RGC axon terminals and that is subject to NMDA receptor activity blockade. These observations, together with the time-course of the response of tectal neurons to BDNF, suggest that this neurotrophin shapes retinotectal synaptic connectivity through a mechanism that differentially influences postsynaptic tectal neurons and presynaptic RGCs.

MATERIALS AND METHODS

Animals

Adult *Xenopus laevis* females were primed with human chorionic gonadotropin (Sigma Aldrich, St Louis MO) to induce egg laying and oocytes were fertilized in vitro. Tadpoles were maintained in modified rearing solution (60 mM NaCl, 0.67 mM KCl, 0.34 mM $Ca(NO_3)_2$, 0.83 mM $MgSO_4$, 10 mM HEPES pH 7.4, 40 mg/l gentamycin) with 0.001% phenylthiocarbamide added to prevent melanocyte pigmentation. During imaging and injections, tadpoles were anesthetized with 0.05% tricane methanesulfonate (Finquel, Argent Laboratories, Redmond, WA). All staging was carried out according to Nieuwkoop and Faber (Nieuwkoop and Faber, 1956), and animal procedures were approved by the Institutional Animal Care and Use Committee at the University of California, Irvine.

PSD95-GFP in vivo expression and dendritic arbor labeling

Xenopus optic tectal neurons were visualized in vivo by methods similar to those previously used for imaging *Xenopus* RGC axons (Alsina et al., 2001). To visualize postsynaptic specializations and tectal neuron morphology simultaneously, brain progenitor cells were co-transfected with expression plasmids containing a chimeric gene encoding GFP and PSD-95 (a gift from Dr D. Bredt, UCSF) and a red fluorescent protein variant (pDsRed2; Clontech, Palo Alto, CA). Stage 20-22 tadpoles were anesthetized and pressure injected into the tectal primordium with 0.1-0.2 nl of 1 μg/μl of each plasmid mixed with the lipofecting agent DOTAP (Boehringer Mannheim, Indianapolis, IN). Tadpoles were reared until stage 45, when those tadpoles with distinct neurons expressing DsRed2 throughout their dendritic arbor and with punctate PSD95-GFP labeling were selected for imaging. In experiments that examined the role of BDNF, 0.2-1.0 nl of recombinant human BDNF (200 ng/μl; Amgen, Thousand Oaks, CA), BDNF function-blocking antibody (330 μg/ml of purified IgG; R&D Systems, Minneapolis, MN), vehicle solution (50% Niu Twitty) or control non-immune IgG was pressure-injected into the ventricle and subpial space surrounding the optic tectum immediately following the first imaging session. In experiments that established synapse and branch dynamics in tadpoles with and without NMDA receptor activity blockade, 0.1 nl of APV (50 μM in vehicle solution; Tocris Cookson, UK) or vehicle solution alone was injected into the optic tectum immediately following the first imaging session. Imaging was performed on a Pascal LSM 5 (Zeiss, Germany) or a Nikon PCM2000 (Melville, NY) laser-scanning confocal microscope equipped with Argon and HeNe lasers as described before (Alsina et al., 2001; Hu et al., 2005). Thin (1.0-1.5 μm) overlapping optical sections encompassing the entire dendritic arbor and cell body were collected simultaneously at the two wavelengths, with minimal gain and contrast enhancements, and at below-saturation levels. Images were acquired immediately prior to injections, and then at various intervals up until 48 hours post-injection.

Immunocytochemistry

For GFP and endogenous SNAP-25 co-localization, tadpoles with neurons expressing PSD95-GFP were anesthetized and fixed by immersion in 2% paraformaldehyde and 3.75% acrolein in 0.1 M phosphate buffer pH 7.4 (PB); the brains were removed and postfixed with the same fixative for 1 hour. Horizontal free-floating vibratome sections (25 μm) were obtained, preincubated in blocking solution (1.5% goat normal serum, 0.1% Triton X-100 in 0.1 M PB), and incubated overnight with mouse anti-GFP (1:100 dilution in 0.1% Triton X-100 in 0.1 M PB; Molecular Probes) and rabbit anti-SNAP25 (1:1,000 dilution; Stressgen Biotechnologies, Victoria, Canada) antibodies simultaneously. For endogenous PSD-95 and SNAP-25 co-localization, stage 45 tadpoles were fixed in 4% paraformaldehyde; 20 μm cryostat sections were obtained and incubated with anti-PSD-95 (mouse IgG, 1:200 dilution; Upstate Biotechnology, Lake Placid, New York) and rabbit anti-SNAP-25 overnight. Tissues were then rinsed and incubated with Alexa 488 anti-mouse and Alexa 568 anti-rabbit antibodies (1:200 dilution each in 0.1 M PB; Molecular Probes, Eugene, OR). All images were collected with a LSM 5 Pascal confocal microscope using a 63×/1.4 NA oil immersion objective. To determine colocalization of fluorescent labels, optical sections were collected at 0.5 μm intervals through the full extent of the PSD95-GFP positive neuron.

Electron microscopy

For electron microscopy immunostaining, 50 μm horizontal vibratome sections were collected in 0.1 M PB. Sections were incubated in 1% sodium borohydrade, cryoprotected in 25% w/v sucrose and quickly permeabilized in liquid nitrogen. Sections were rinsed, incubated in blocking solution (0.5% BSA in 0.1 M TBS), and incubated overnight with a mouse monoclonal anti-GFP antibody (1:10 dilution in 0.1% BSA in 0.1 M TBS) followed by a secondary goat anti-mouse IgG coupled to 1 nm gold particles (1:50 dilution in 0.5% fish gelatin, 0.8% BSA in 0.01 M PBS, pH 7.4; Aurion-EMS, Hatfield, PA). Gold particles were enlarged using a British BioCell silver intensification kit (Ted Pella, Redding, CA) and sections were post-fixed and processed for electron microscopy as described before (Hu et al., 2005). Ultrastructural analysis was performed using a Phillips CM20 transmission electron microscope.

Data analysis

Data analysis was similar to that described by Hu et al. (Hu et al., 2005) for RGC axon arbors. All analysis was performed from raw confocal images without any post-acquisition manipulation or thresholding. Digital three-dimensional reconstructions of DsRed2-labeled dendritic arbors (red only) were extracted from a stack of optical sections covering the entire extent of the arbor with the aid of the MetaMorph software (Universal Imaging, West Chester, PA). Pixel-by-pixel overlaps from individual optical sections obtained at the two wavelengths were analyzed to determine the identity and position of PSD95-GFP puncta along the dendritic arbor. Discrete PSD95-GFP labeled puncta of 0.5-1.0 μm^2 in size (size of smallest puncta) with median pixel values 2.0-3.0 times greater than the median pixel values of background non-punctate GFP within the same dendritic arbor were considered to be single synaptic puncta. During data analysis, care was taken to ensure that similar ratios were maintained for every neuron analyzed throughout the 48-hour observation period. Any continuous, non-punctate GFP fluorescence in the cell body and proximal region of a primary dendrite was excluded from the analysis.

Several parameters were measured to obtain a detailed analysis of PSD95-GFP puncta dynamics at each observation interval: the number of puncta per branch or per unit arbor length, the number of puncta added or eliminated, the number of puncta maintained from one observation to the next, and the location of each PSD95-GFP puncta along the dendritic arbor. Total dendritic arbor length (length of total branches), total branch number, the number of individual branches gained or lost and the number of branches remaining from one observation to the next were measured for the quantitative analysis of dendrite branching. Extensions of more than 5 μm were classified as branches. Total arbor length was measured from binarized images of the digitally reconstructed neurons. A relative measure of cumulative length of all branches per dendritic arbor was obtained by counting total pixel number from the proximalmost part of the primary

dendrite. Neurons imaged were from the mid-region of the optic tectum and had between 11 and 37 branches for control (x=21, 20 neurons), 10 and 41 for BDNF (x=17, 16), and 12 and 40 in anti-BDNF treated tadpoles (x=27, 12). Data are presented as percent increase from the initial observation interval to each subsequent interval, or as percent increase for each observation interval. Two-sample unpaired t-tests and one-way ANOVA Tukey's multiple comparison tests (Systat, SPSS) were used for the statistical analysis of data and significance was $*P \leqslant 0.05$; $**P \leqslant 0.005$. Data are presented as mean±standard error of the mean (s.e.m.).

In control experiments, we examined potential effects of BDNF on *Xenopus* tectal neuron morphology by altering BDNF tectal levels prior to peak endogenous tectal BDNF expression. Stage 40/42 *Xenopus* tadpoles with individual tectal neurons expressing DsRed2 were selected and microinjected with BDNF (either in solution or coupled to green fluorescent microspheres), or with vehicle solution or cytochrome C-treated microspheres, as described by Lom and Cohen-Cory (Lom and Cohen-Cory, 1999). Total dendrite number and complexity were analyzed 48 hours after treatment, at stage 43/44. Tectal neurons in tadpoles treated with BDNF in solution or coupled to beads had similar dendritic arbor morphologies as neurons in control-treated tadpoles. Tectal neurons in the BDNF-treated tadpoles had an average of 11.48±0.92 branch tips (48 neurons), while in controls, tectal neurons had 11.84±1.1 branch tips (37 neurons) 48 hours after treatment. Thus, although under the same experimental conditions, BDNF significantly affects RGC dendritic and axonal arborization (Alsina et al., 2001; Lom et al., 2002), no significant effects were observed on tectal neuron primary dendrite number or total branch tip number (P=0.803).

RESULTS

We used in vivo time-lapse confocal microscopy to image synaptic sites in tectal neuron dendritic arbors and to examine mechanisms involved in the establishment of *Xenopus* retinotectal synaptic connectivity. Expression of DsRed2 and the postsynaptic density protein PSD95 tagged with GFP (PSD95-GFP) was used to visualize dendritic arbor morphology and postsynaptic specializations simultaneously in vivo (Fig. 1). PSD-95 associates with postsynaptic receptors and cytoskeletal elements, participates in synapse maturation, and has served as a marker for imaging postsynaptic specializations both in culture and in vivo (Ebihara et al., 2003; Marrs et al., 2001; Niell et al., 2004; Okabe et al., 2001). In *Xenopus* optic tectum, PSD95-GFP had a punctate distribution along individual DsRed2-labeled tectal neuron dendritic arbors (Fig. 1A-C). To confirm that PSD95-GFP was correctly targeted to postsynaptic sites in vivo, we compared PSD95-GFP distribution with that of an endogenous presynaptic protein. Immunostaining for the presynaptic plasma membrane protein SNAP-25 showed that, in the tectal neuropil, endogenous SNAP-25 is distributed in a punctate pattern that is complementary to that of PSD95-GFP punctate labeling (Fig. 1D-G) and of endogenous PSD-95 staining (Fig. 1H-J). Most of the PSD95-GFP puncta co-localized with endogenous SNAP-25 punctate staining (81.25±3.12%, 357 puncta analyzed from five neurons, one PSD95-GFP neuron per tadpole), indicating that PSD95-GFP targets to synaptic sites. Specific localization of PSD95-GFP at synapses was also confirmed ultrastructurally. Immunoelectron microscopy demonstrates that PSD95-GFP predominantly localized to the postsynaptic side of mature synaptic profiles in the tectal neuropil of stage 45 tadpoles (Fig. 2). Morphologically mature synapses with presynaptic terminals containing numerous synaptic vesicles and clearly defined postsynaptic specializations were immunopositive for GFP. In most immunopositive profiles (84.8%, or 28 out of 33 profiles analyzed

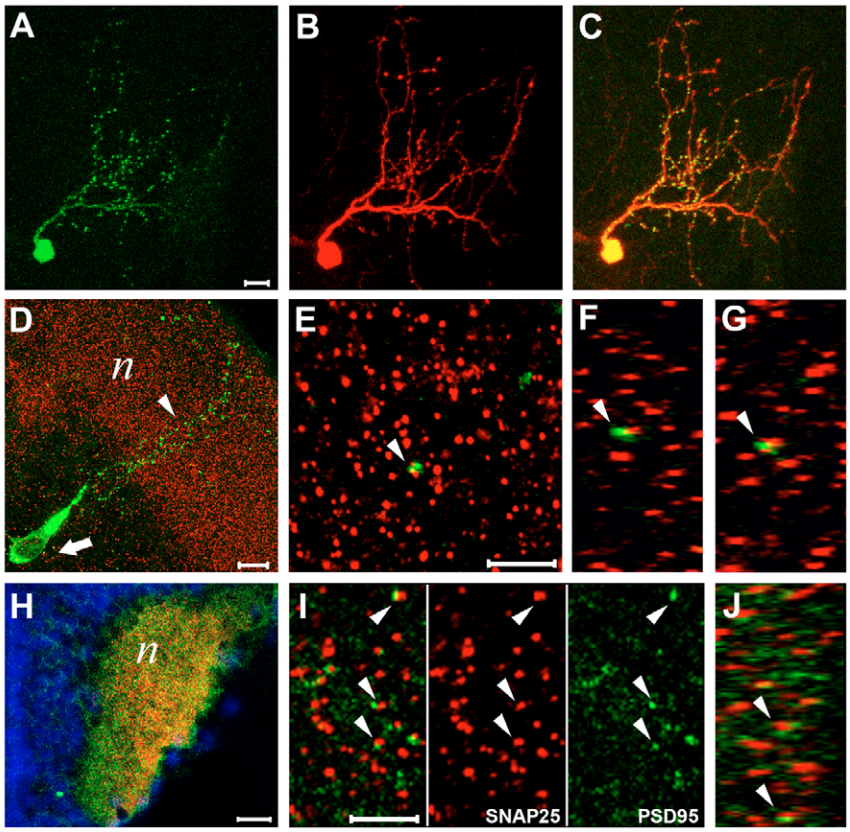

Fig. 1. PSD95-GFP localizes to synaptic contact sites in vivo. (**A-C**) Confocal image of a tectal neuron double-labeled with (A) PSD95-GFP and (B) DsRed2 shows the punctate distribution of PSDS95-GFP along the dendritic arbor and in terminal branches (C, overlay). (**D-G**) Co-localization between PSD95-GFP and endogenous SNAP-25 expression in stage 45 tadpoles. (D) A PSD95-GFP labeled tectal neuron (arrow indicates cell body; arrowhead indicates dendritic arbor) and the distribution of endogenous SNAP-25 in the tectal neuropil (n) are shown by the low-magnification confocal image of a tadpole brain section. (E) A single plane, high-magnification image illustrates the discrete distribution and co-localization of PSD95-GFP puncta with SNAP-25 immunostaining. (F,G) The spatial coincidence and close apposition between the PSD95-GFP and SNAP-25 is clearly illustrated in the (F) x-z and (G) y-z orthogonal planes (arrowheads) of the coincident puncta shown in E (arrowhead). The GFP and SNAP-25 puncta are adjacent rather than completely coincident, owing to the localization of SNAP-25 and PSD95-GFP in pre- and post-synaptic membranes, respectively. (**H-J**) Co-localization between endogenous SNAP-25 and PSD-95 proteins. (H) A transverse cryostat section shows SNAP-25 (red) and PSD-95 (green) immunostaining in the tectal neuropil of a stage 45 tadpole. Cell bodies are revealed by the DAPI staining (blue). (I,J) Co-localization and punctate distribution of endogenous SNAP-25 and PSD-95 is illustrated by: (I) the overlaid image of a single, high-magnification confocal plane and its two individual components; and (J) an overlaid, x-z orthogonal plane. Most endogenous SNAP-25 and PSD-95 puncta are apposed (examples shown by the arrowheads); 87.9±3.07% of SNAP-25 puncta were apposed by PSD-95 puncta (2139 puncta from 10 individual sections analyzed). Scale bars: 10 μm for A-D; 20 μm for H; 5 μm E-G,I,J.

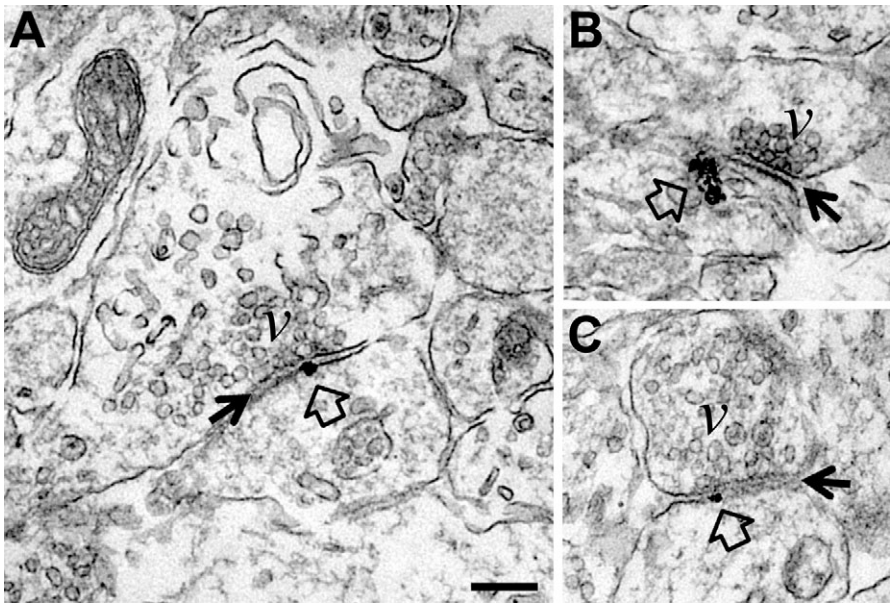

Fig. 2. PSD95-GFP specifically localizes to ultrastructurally identified synapses on tectal neuron dendrites. (**A-C**) The localization of PSD95-GFP was determined by examining the distribution of GFP immunoreactivity by electron microscopy. The electron photomicrographs show specific localization of GFP immunoreactivity as revealed by the silver-enhanced gold particles (open arrows) at postsynaptic terminals. Morphologically mature synapses (black arrows), containing presynaptic terminals with numerous synaptic vesicles (v) and clearly defined pre- and postsynaptic specializations are observed. The silver enhanced gold particles were directly localized to the postsynaptic membrane at the postsynaptic density (A-C), or were within 200 nm of the postsynaptic density (B). Scale bar: 200 nm.

from seven brains, one PSD95-GFP neuron per tadpole brain), the GFP immunoreactivity was localized at or near the postsynaptic density at the synapse (Fig. 2A-C). Therefore, these studies directly demonstrate that PSD95-GFP is recruited to synapses, and validate it as a marker to visualize postsynaptic sites in vivo.

Time-lapse imaging of PSD95-GFP puncta in individual DsRed2-labeled tectal neuron dendritic arbors was used to correlate dendritic arbor morphology with synapse formation and stabilization. Our previous studies show that BDNF significantly increases the number of presynaptic specializations and the complexity of RGC axon arbors in stage 45 *Xenopus* tadpoles within 4 hours of treatment (Alsina et al., 2001). At this stage, endogenous BDNF levels in the optic tectum are high (Cohen-Cory and Fraser, 1994), and tectal neurons increase their complexity by an active remodeling of their dendritic arbors (Cline, 1998; Cline, 2001; Wu and Cline, 1998). Therefore, stage 45 tadpoles were imaged by confocal microscopy at 0, 4, 24 and 48 hours to determine potential effects of BDNF on tectal neurons. Microinjection of recombinant BDNF into the optic tectum did not alter the growth or morphology of tectal neuron dendritic arbors imaged at any of the observation time points when compared with controls (Fig. 3 and Fig. 4A,B). Similarly, BDNF did not influence dendritic arbor complexity of neurons in young tadpoles (prior to peak BDNF expression) imaged 48 hours post-treatment (see Materials and methods) nor the branching of tectal neurons imaged on a time-course of once every 2 hours (data not shown). By contrast, BDNF treatment significantly increased the number of PSD95-GFP-labeled postsynaptic specializations per individual arbor (Fig. 3 and Fig. 4C,D). Quantitative analysis of individual arbors demonstrates that the total number and density of PSD95-GFP puncta per tectal neuron dendritic arbor were significantly increased 24 hours after BDNF treatment when compared with controls (Fig. 4C,D). The difference in the number and density of PSD95-GFP puncta became more dramatic by 48 hours (Fig. 4C,D).

Our previous studies demonstrate a dual function for BDNF during the formation and stabilization of both synapses and axon branches in *Xenopus* RGC arbors (Alsina et al., 2001; Hu et al., 2005). Increasing BDNF within the tadpole optic tectum induces new axon branches and presynaptic specializations to be formed while decreasing endogenous BDNF induces the destabilization of both presynaptic sites and axon branches. These observations suggest that limiting amounts of BDNF dictate the extent of axon arbor growth and stabilization. Thus, to determine whether the effects of recombinant BDNF on tectal dendrites reflect the actions of endogenous BDNF, we decreased endogenous BDNF levels by injecting a BDNF function-blocking antibody into the optic tectum. As observed for recombinant BDNF, the anti-BDNF treatment did not alter dendritic branch number at any observation interval (4, 24 or 48 hours; Fig. 3D). Total branch number was similar for tectal neurons in control, BDNF, and anti-BDNF treated tadpoles (Fig. 4A), indicating that dendritic branching was unaffected by alterations in BDNF signaling. However, neutralizing endogenous BDNF did limit the spatial extent of the dendritic arbor. Total dendritic arbor length remained constant in tectal neurons in anti-BDNF treated tadpoles throughout the 48-hour observation period (105.2±9% of time zero, 6; Fig. 4B), while in controls, total dendrite arbor length increased to 153.5±15% of its initial value by 48 hours ($P \leqslant 0.05$). Neutralizing endogenous BDNF with anti-BDNF had opposite effects on GFP-labeled postsynaptic specializations to those of recombinant BDNF, significantly decreasing the number of PSD95-GFP puncta in the tectal dendrites (Fig. 3D). The total number of PSD95-GFP puncta per tectal neuron was significantly lower than controls 24 hours after anti-BDNF treatment, an effect that became more pronounced by 48 hours (Fig. 4C). Because neutralization of endogenous BDNF influenced the length of the dendritic arbor and the number of PSD95-GFP puncta, when normalized, the number of postsynaptic specializations per unit arbor length (postsynaptic specialization density; Fig. 4D) did not differ significantly from control, although the two parameters were affected independently. Time-lapse analysis revealed, however, that the decrease in the absolute number of PSD95-GFP puncta in the anti-BDNF-treated tadpoles resulted in a significant decrease in the density of postsynaptic specializations in branches that remained stable over time (Fig. 5). Thus, like treatment with recombinant BDNF, neutralizing endogenous BDNF within the optic tectum affected postsynaptic specialization number in tectal neuron dendritic arbors.

Detailed analysis of the localization and the lifetimes of individual PSD95-GFP puncta per dendritic arbor revealed that the effect of BDNF on synapse density was due to the selective addition of new

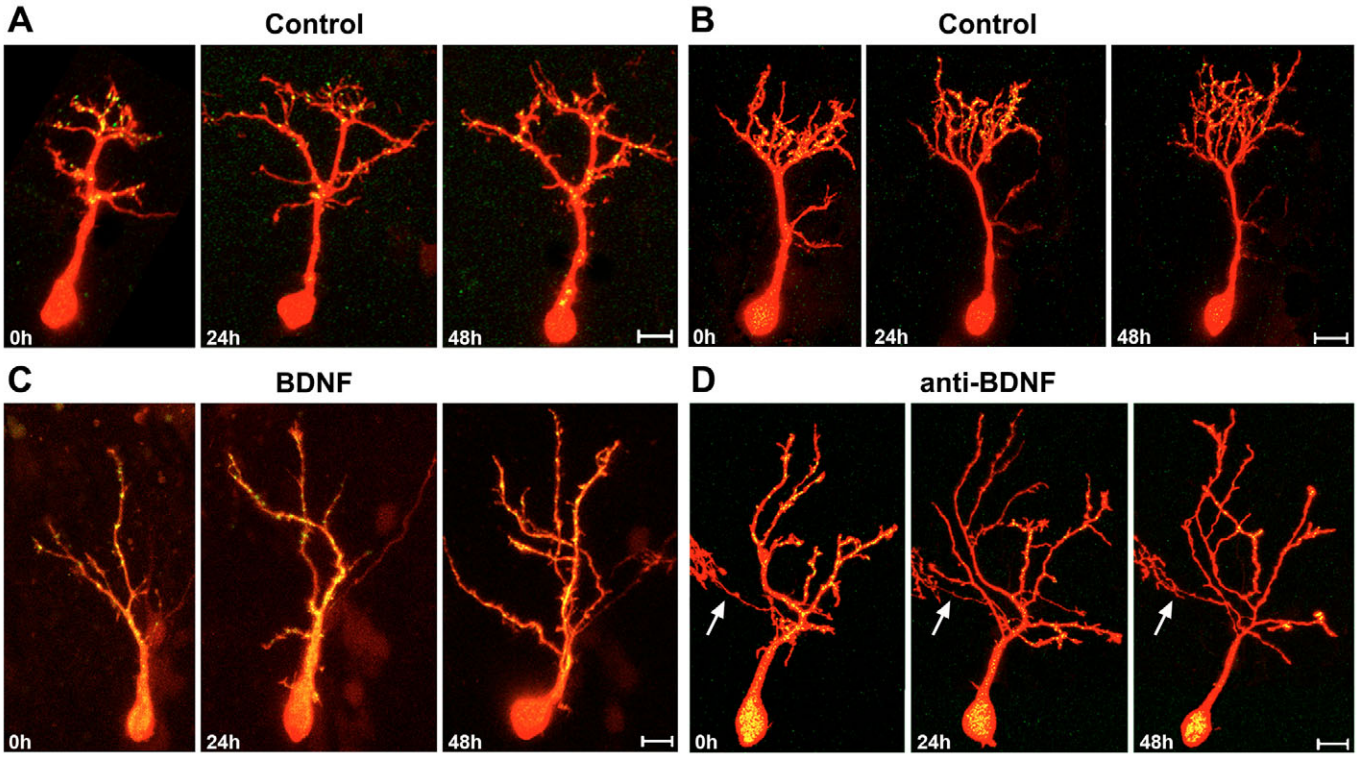

Fig. 3. Manipulations in BDNF tectal levels influence PSD95-GFP labeled postsynaptic specializations on tectal neuron dendritic arbors. Image reconstructions of representative tectal neurons illustrate dendritic arbor complexity and synapse number 0, 24 and 48 hours after BDNF or anti-BDNF treatment. Individual neurons double labeled with PSD95-GFP and DsRed2 were visualized by confocal microscopy in live developing tadpoles after acute tectal injection of (**A**,**B**) control vehicle solution, (**C**) BDNF or (**D**) anti-BDNF. (A-D) Tectal neuron dendritic arbors become morphologically more complex over time. (C) In the BDNF-treated tadpoles, both the number and density of PSD95-GFP puncta per dendrite increased at 24 and 48 hours. (D) Anti-BDNF limited dendritic arbor growth and decreased PSD95-GFP puncta (see also Figs 4, 5). The arrow indicates the axonal process of the neuron. Scale bars: 20 μm.

postsynaptic specializations rather than stabilization of existing ones (Fig. 6). The BDNF-elicited increase in synapse addition occurred between 4 and 24 hours after treatment (Fig. 6B). Conversely, the anti-BDNF-elicited decrease in synapse number was the result of a reduced amount of newly added postsynaptic specializations. That is, significantly fewer PSD95-GFP puncta were formed by 48 hours following anti-BDNF treatment, a trend that was observed from 4 hours onwards (Fig. 6B). The proportion of PSD95-GFP puncta that remained stable in neurons in BDNF and in anti-BDNF treated tadpoles was similar to that of controls at all observation intervals (Fig. 6A). Together, our results demonstrate that alterations in tectal BDNF levels do not influence tectal neuron dendritic arbor morphology but rather influence synapse density by modulating synapse formation.

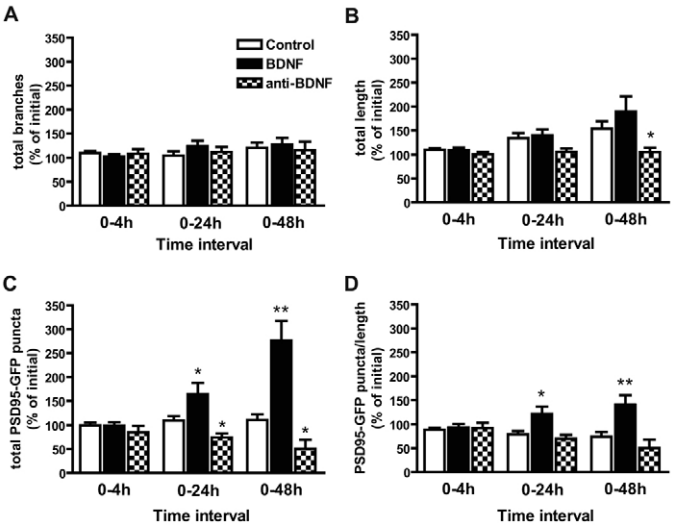

Fig. 4. BDNF influences postsynaptic specializations on tectal neurons without altering dendritic arbor morphology. The effects of BDNF and anti-BDNF treatment on (**A**) dendrite branch number, (**B**) total dendritic arbor length, and (**C**) number and (**D**) density of PSD95-GFP-labeled postsynaptic specialization are expressed as percent change from their initial value at the time of treatment. (A) Total dendrite branch number was similar for tectal neurons in control, BDNF and anti-BDNF treated tadpoles at all observation time points. (B) A similar relative increase in total dendritic arbor length, a measure of dendrite branch number and the spatial extent of all branches, was observed in control and BDNF-treated tadpoles at all observation time points. By contrast, total dendritic arbor length remained close to its initial value at all observation time points after anti-BDNF treatment. (C,D) BDNF significantly increased (C) the number and (D) density of PSD95-GFP puncta per dendritic arbor 24 hours after treatment, an effect that was strengthened and maintained for 48 hours. (C,D) Anti-BDNF significantly decreased PSD95-GFP puncta number by 24 hours but did not influence puncta number per unit arbor length. Bars indicate s.e.m. n=18 neurons in control, n=16 neurons in BDNF and n=12 neurons in anti-BDNF. *$P \leqslant 0.05$, **$P \leqslant 0.005$ compared with control.

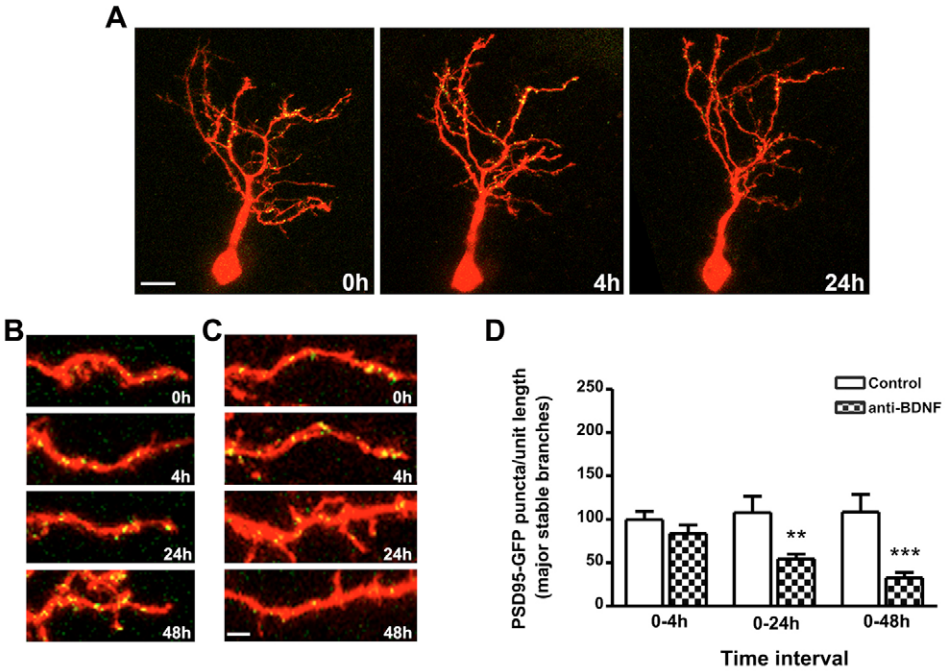

Fig. 5. Anti-BDNF decreases synapse density per dendrite branch. (**A**) Reconstructions of a sample tectal neuron imaged at 0, 4 and 24 hours further illustrate the onset of anti-BDNF effects on postsynaptic specialization density and dendritic arbor morphology. Scale bar: 20 μm. (**B**,**C**) High-magnification images of individual dendritic branches in (B) control and (C) anti-BDNF treated tadpoles compare changes in PSD95-GFP puncta per branch, over the 48 hour imaging period. Scale bar: 5 μm. (**D**) A measure of the effects of anti-BDNF on postsynaptic specialization density per branch was obtained by counting the number of PSD95-GFP puncta at each observation interval in branches with lifetimes of more than 48 hours (that were present at all observation time points, from 0 to 48 hours). Data were normalized for the change in branch length and are presented as the percent of its initial value at the time of treatment compared with control. Bars indicate s.e.m. n=25 branches in control and n=25 in anti-BDNF. *P≤0.05, **P≤ 0.005 compared with control.

Our results show that the effects of altering tectal BDNF levels on dendritic arbor growth and synapse dynamics differ from the effects of similar manipulations on presynaptic RGC axon arbors (Alsina et al., 2001; Hu et al., 2005). It was therefore important to determine whether presynaptic events correlate with changes in postsynaptic tectal neurons and whether other manipulations that affect presynaptic axons would have similar or differential effects on postsynaptic neurons. Time-lapse imaging of tectal neurons every 2 hours for a period of 8 hours (Fig. 7A) was used to correlate dendrite and postsynaptic site dynamics with RGC axon branch dynamics. Time-lapse imaging demonstrates that branch lifetimes of tectal neuron dendritic arbors closely resemble those of presynaptic RGC axon arbors. An average of 70.1±3.9% dendritic branches remained stable and 34.5±5.7% branches were added over each 2-hour period (five neurons; one neuron per tadpole, Fig. 7D). Likewise, 73.3±1.6% axon branches are stable and 32.7±2.8% branches are added on RGC axon arbors similarly imaged every 2 hours (Alsina et al., 2001; Hu et al., 2005).

To relate synapse dynamics to dendrite branch dynamics, we determined the number and distribution of PSD95-GFP puncta in the individual tectal neuron dendritic arbors (see Materials and methods). PSD95-GFP puncta were distributed along proximal and distal dendrites (Fig. 7A, and see also Fig. 1C), with a significant number of branch points containing PSD95-GFP puncta (72.3±2.3%; not shown graphically; see Fig. 7B,C). Time-lapse analysis also revealed that a significant fraction of the PSD95-GFP puncta on the dendritic arbors had lifetimes of more than 2 hours (an average of 76.4±3.3% puncta remained stable from one two-hour observation to the next; Fig. 7E). As dendrites branched, new PSD95-GFP puncta appeared at previously unlabeled locations, presumably indicating new synaptic contacts. An average of 30.8±6.0% PSD95-GFP puncta were added from one 2-hour observation interval to the next (Fig. 7E), resulting in a net increase of postsynaptic specializations over time. Much like branch

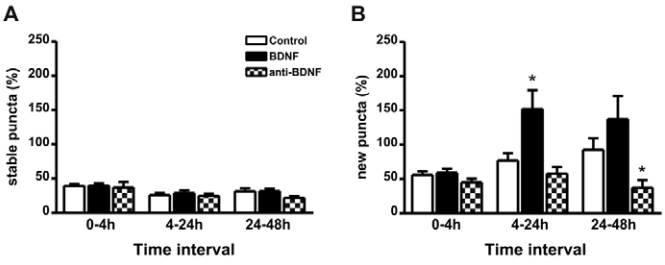

Fig. 6. BDNF increases synapse density in tectal neuron dendritic arbors by promoting synapse formation. (**A**) The number of PSD95-GFP-labeled postsynaptic specializations that remained stable from one observation interval to the next (0-4; 4-24; 24-48 hours) in tectal neuron dendritic arbors was similar for control, BDNF- and anti-BDNF-treated tadpoles. (**B**) BDNF increased the proportion of new PSD95-GFP-labeled postsynaptic specializations that are formed, an effect that primarily takes place between 4 and 24 hours after treatment. Conversely, neutralization of endogenous BDNF with anti-BDNF decreased the number of new PSD95-GFP puncta formed, most significantly between 24 and 48 hours after treatment. Bars indicate s.e.m. n=18 neurons in control, n=16 neurons in BDNF and n=12 neurons in anti-BDNF. *P≤0.05, **P≤0.005 compared with control.

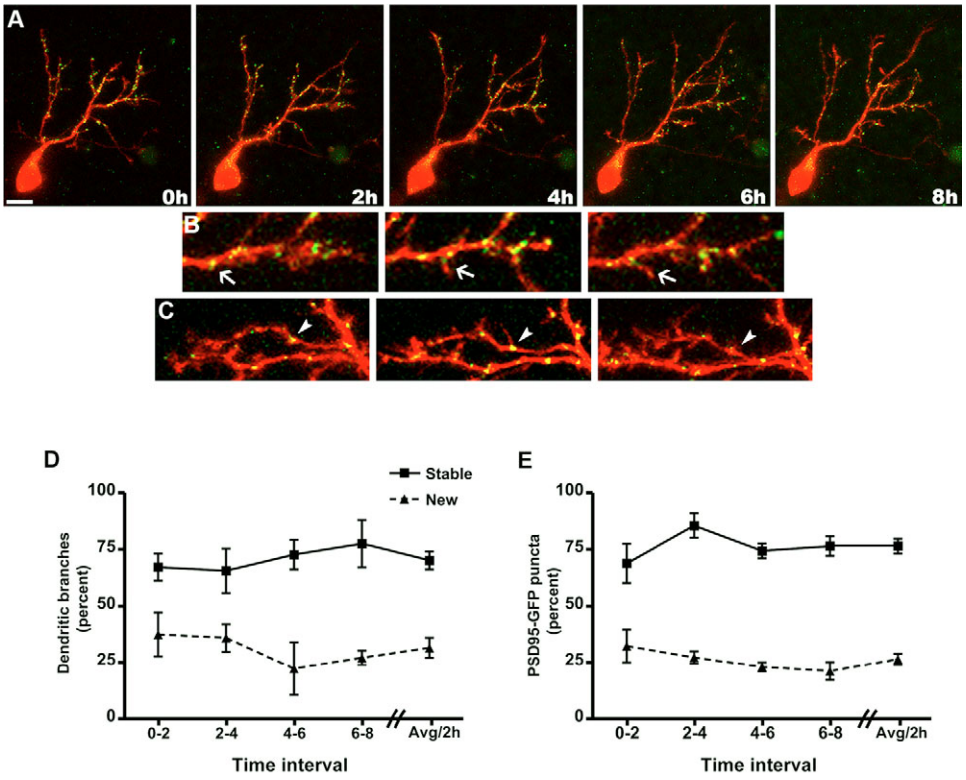

Fig. 7. Dendrite branch and postsynaptic specialization dynamics in individual tectal neuron dendritic arbors. Time-lapse confocal imaging of neurons expressing DsRed2 and PSD95-GFP illustrates postsynaptic site and dendritic branch dynamics. (**A**) Image reconstructions of a tectal neuron illustrates the localization and distribution of PSD95-GFP puncta (yellow) within specific regions of the arborizing, DsRed-labeled dendritic arbors (red). (**B**,**C**) Magnified regions of two dendritic arbors show that transient (arrowhead) and stable (arrows) branches appear at arbor sites where PSD95-GFP puncta localize. A significant number of branch points (72.3±2.3%) contained PSD95-GFP puncta (not shown graphically). (**D**,**E**) Detailed analysis of number and distribution of PSD95-GFP-labeled puncta per arbor illustrates the relationship between synapse and dendritic branch dynamics. The number of branches and PSD95-GFP puncta that remained from one 2-hour observation interval to the next (stable puncta), and the number of new branches and PSD95-GFP puncta added between observation intervals was calculated and normalized for each time interval to obtain a dynamic measure of branch and synapse addition and stabilization over time. (D) An average of 70.1±3.9% branches were stable and 34.5±5.7% branches were added at each 2-hour observation interval. (E) Most PSD95-GFP puncta per dendritic arbor were stable; an average of 76.4±3.3% puncta remained at the same location from one observation interval to the next and 30.8±6.0% new puncta appeared at each 2-hour observation interval. Symbols indicate means±s.e.m.; *n*=5 neurons in five tadpoles.

dynamics, the proportion of new and stable postsynaptic specializations on tectal dendritic arbors closely resembled the proportion of new and stable presynaptic specializations on RGC axon arbors, where 69±1.5% of GFP-synaptobrevin labeled presynaptic specializations are stable and 37.1±3.6% of the presynaptic specializations are added every 2 hours (Alsina et al., 2001; Hu et al., 2005). Together, these observations indicate that in the *Xenopus* retinotectal system, axonal and dendritic branching and pre- and postsynaptic site elaboration are related.

Blockade of the NMDA receptor, a glutamate receptor that mediates the major mode of synaptic transmission at *Xenopus* retinotectal synapses, has been shown to influence the dynamic behavior of both RGC axon and tectal neuron dendritic arbors in the short term (Rajan and Cline, 1998; Rajan et al., 1999). Our previous work demonstrates that altering NMDA receptor activity in the optic tectum of developing tadpoles significantly influences presynaptic site stabilization in RGC axon arbors (Hu et al., 2005). The number of GFP-synaptobrevin-labeled presynaptic specializations is significantly reduced to less than 50% of its initial value in RGC axon arbors within 2 hours of blocking NMDA receptors, a treatment that also influences axon arbor morphology by 24 hours (Hu et al., 2005). Analysis of PSD95-GFP puncta and dendrite branch number in tectal neurons of stage 45 tadpoles microinjected with APV shows that the decrease in synapse number in RGC axon arbors is paralleled by a significant decrease in the number of postsynaptic specializations in the dendritic arbors (Fig. 8) (see also Hu et al., 2005). The number of PSD95-GFP-labeled postsynaptic specializations in tectal neurons exposed to APV decreased to less than 50% of controls 2 hours after treatment, a reduction that became more significant by 24 hours (Fig. 8A). Only a delayed effect on dendritic branch number was observed at 24 hours (Fig. 8C), similar to the impact of NMDAR blockade on RGC axon arbor morphology that we previously reported [Fig. 8D, adapted, with permission, from Hu et al. (Hu et al., 2005)]. Consequently, in vivo imaging reveals coincident mechanisms of synaptogenesis, and pre- and postsynaptic arbor growth that are similarly influenced by NMDA receptor activity. These coordinated, activity-dependent changes in synaptic connectivity further underscore the differential action of BDNF on presynaptic RGC axons and postsynaptic tectal neurons.

DISCUSSION

In this study, we used in vivo time-lapse imaging and analysis of PSD95-GFP-labeled postsynaptic specializations in tectal neuron dendritic arbors to explore dynamic mechanisms of retinotectal

connectivity and to examine further the participation of BDNF in this process. One of the earliest events in postsynaptic differentiation is the recruitment of scaffolding proteins, including PSD95 (Friedman et al., 2000; Okabe et al., 2001). Our studies provide direct ultrastructural evidence that PSD95-GFP is transported and is specifically localized to morphologically mature synapses in the *Xenopus* visual system, therefore validating its use as a dynamic marker to study the development of synaptic connectivity (Ebihara et al., 2003; Marrs et al., 2001; Niell et al., 2004; Okabe et al., 2001). By using PSD95-GFP to label synapses, our in vivo imaging studies revealed a direct correlation between the dynamic remodeling of synapses and dendritic arbor structure: in *Xenopus*, as in zebrafish (Niell et al., 2004), the active formation and stabilization of PSD95-GFP labeled synaptic sites is related to the dynamic branching of tectal neuron dendritic arbors. Furthermore, our studies demonstrate that the branching and synaptic complexity of *Xenopus* tectal neuron dendritic arbors is closely related to the dynamic branching and synaptic complexity of presynaptic RGC axon arbors. Two-hour time lapse imaging of PSD95-GFP labeled postsynaptic specializations and dendrite branch dynamics demonstrates that synapse formation and stabilization in tectal neuron dendritic arbors parallels the behavior of RGC axon arbors imaged at the same developmental stage and at similar time intervals [as shown in Fig. 7 and by Alsina et al. (Alsina et al., 2001)]. In vivo imaging studies also demonstrate that manipulations that can directly influence synaptic interactions (for example, by blocking retinotectal synaptic transmission with APV) have analogous effects on branch and synapse dynamics in both RGC axons and tectal neuron dendrites. Thus, our results are consistent with the coordinated growth and motility of pre- and postsynaptic components, as observed for neurons establishing synapses in culture systems (Konur and Yuste, 2004; Umeda et al., 2005). It will be of great significance to observe and confirm these coordinated, dynamic events of synaptogenesis and axon and dendritic branching in pairs of RGCs and tectal neurons that contact one another directly in vivo.

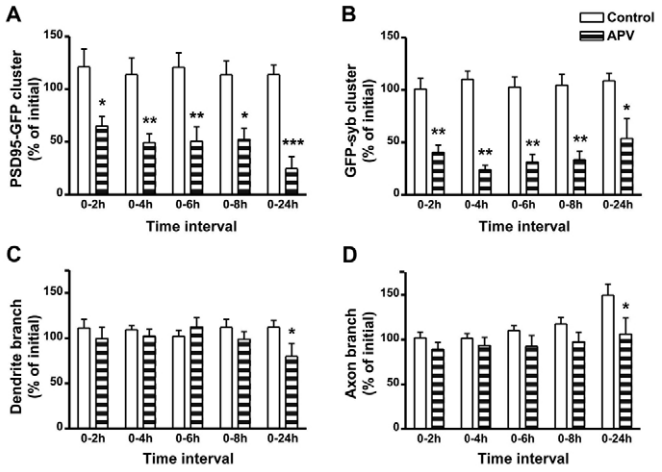

Fig. 8. NMDA receptor blockade equally affects pre- and postsynaptic specializations on RGC axon and tectal neuron dendritic arbors. The effects of altering NMDAR transmission in the optic tectum on PSD95-GFP labeled postsynaptic specializations in tectal neuron dendritic arbors is compared with the effects of the same treatment on GFP-synaptobrevin-labeled presynaptic specializations on RGC axon arbors (see Hu et al., 2005). PSD95-GFP puncta and dendrite branch number in tadpoles that received a single tectal injection of APV is shown as the percent change from their initial value at the time of treatment. (**A**) APV significantly decreased the number of PSD95-GFP puncta compared with control 2 hours after treatment, an effect that was maintained for 24 hours. (**B**) A more dramatic decrease in GFP-synaptobrevin cluster number was observed 2 hours after APV treatment, with a peak cumulative effect occurring after 4 hours [adapted from Hu et al. (Hu et al., 2005)]. (**C**) Dendritic arbor complexity, expressed as the increase in total branch number per dendritic terminal, is affected by the APV treatment by 24 hours only. (**D**) Similar to dendrite branch number, the APV treatment had a significant effect on RGC axon branch number by 24 hours only [adapted, with permission, from Hu et al. (Hu et al., 2005)]. Bars indicate mean±s.e.m. For tectal neurons, n=5 in control and n=9 in APV-treated tadpoles. For RGC axons, n=14 in control and n=10 in APV-treated tadpoles. $*P \leqslant 0.05$; $**P \leqslant 0.005$ compared with control.

The rapid dynamic extension and elimination of dendritic filopodia or short branches is a common process during the growth and remodeling of dendritic arbors (Rajan et al., 1999). It is only through the gradual accumulation of new branches and the lengthening of pre-existing branches that the dendritic arbor grows to attain a more complex morphology (Cline, 2001). In vivo time-lapse imaging in zebrafish previously characterized two populations of postsynaptic specializations in tectal neuron dendritic arbors (Niell et al., 2004): a large population of PSD95-GFP puncta that is highly dynamic, with lifetimes of less than 20 minutes; and a smaller, stable population with lifetimes of hours. Transient puncta with lifetimes of minutes are thought to correspond to nascent synapses that are susceptible to quick elimination, as are the transient filopodia that often bear these transient synapses (Cline, 2001; Niell et al., 2004). Our analysis focused on the long-term dynamic events that affect tectal neuron dendritic morphology and thus predominantly considered the more stable population of postsynaptic specializations in these neurons.

Manipulations that increased or decreased BDNF levels were used to explore the influence of BDNF on tectal neurons and to help establish a mechanism by which BDNF shapes retinotectal connectivity. Altering endogenous BDNF levels within the *Xenopus* optic tectum influenced tectal neuron synaptic connectivity but did not significantly reshape dendritic arbor morphology. The effects of BDNF and anti-BDNF on synapse number emerged several hours after treatment, becoming significant only by 24 hours. A BDNF-elicited increase in both the number and density of postsynaptic specializations on tectal neurons paralleled, with a relative time-delay, the previously observed increase in presynaptic specializations on RGC axons (Alsina et al., 2001; Hu et al., 2005). Twenty-four hours after exposure to BDNF, the density of GFP-labeled synaptic specializations increased in both the pre- and postsynaptic arbors, reaching ~55% and 34% greater density, respectively, than in RGC axons and tectal neuron dendrites in control tadpoles. Illustrating the difference in the temporal dynamics of the effects of BDNF on RGCs and tectal neurons, postsynaptic specialization number and density in BDNF-treated tectal neurons continued to increase, requiring 48 hours to attain levels similar to those of presynaptic specializations in RGC axons after 24 hours [276.5±40% increase in PSD95-GFP puncta by 48 hours, Fig. 4C; versus 285±43.5% increase in GFP-synaptobrevin puncta by 24 hours (Alsina et al., 2001)]. Likewise, synapse number was similarly decreased both pre- and postsynaptically when endogenous BDNF was neutralized in vivo; more rapidly in RGC axons than in tectal neuron dendrites (Hu et al., 2005) (present results). Together, these data support the idea that experimentally manipulating BDNF levels can reflect the endogenous actions of BDNF. Moreover, the delayed onset of the response of tectal neurons to alterations in BDNF levels (4 to 24 hours) when compared with the rapid response by RGC axons (2-4 hours) suggests that the effects of BDNF on tectal neuron

synapse number are either direct but delayed, or induced in response to the modulation by BDNF of RGC presynaptic differentiation and axon arbor growth.

Neurotrophins, and in particular BDNF, are potent modulators of dendritic development, differentially influencing multiple neuronal populations. Neurotrophins act positively to promote dendritic branching (Horch and Katz, 2002; McAllister et al., 1995; Wirth et al., 2003) but they can also limit the size of the dendritic arbor of a neuron (Lom et al., 2002; Lom and Cohen-Cory, 1999; McAllister et al., 1997). Neurotrophins can act in anterograde, autocrine or paracrine manners to modulate dendritic growth (Baquet et al., 2004; Horch and Katz, 2002; Wirth et al., 2003). Alterations in dendritic arbor morphology by neurotrophins have therefore been taken to imply direct effects on neuronal connectivity (Cline, 2001). Surprisingly, our studies show that alterations that significantly impact synapse number may not always influence dendritic branching, as arbor morphology was essentially unchanged by manipulations in BDNF levels. The observation that dendritic arbors continued to branch but failed to lengthen as a consequence of decreased tectal BDNF levels suggest that BDNF-elicited expansion and enhanced stability of presynaptic RGC arbors is responsible for the observed increases in tectal neuron synaptic connectivity. Observations that tectal neurons overexpressing a dominant negative form of the TrkB receptor have similar dendritic arbor morphologies and dendritic branching and growth rates to neurons in age-matched control tadpoles (S. Marshak and S.C.C., unpublished) support the interpretation that changes in tectal neuron arbor growth in response to anti-BDNF treatment are secondary to effects on presynaptic RGCs.

Target-derived release of neurotrophins and activation of presynaptic receptors has been considered a key mechanism of neurotrophin signaling (Zweifel et al., 2005). However, work over the last few years has shown that presynaptic neurotrophin release and activation of postsynaptic Trk receptors is also a common mechanism by which neurotrophins can regulate synaptic structure and function. In postsynaptic neurons, TrkB signaling modulates neurotransmitter receptor expression and function, induces depolarization and increases synaptic transmission (Elmariah et al., 2004; Ji et al., 2005; Kafitz et al., 1999; Kovalchuk et al., 2002; Luikart et al., 2005). Our observations that BDNF exerts coordinated, although delayed, effects on synaptogenesis, while it differentially influences axon and dendritic arbor structure, are consistent with BDNF acting presynaptically at retinotectal synapses. BDNF-elicited presynaptic structural modifications are also consistent with physiological evidence that BDNF potentiates retinotectal synapses by enhancing neurotransmitter release rather than by increasing postsynaptic response to RGC electrical stimulation (Du and Poo, 2004). It remains possible, however, that BDNF influences postsynaptic differentiation and/or other aspects of tectal neuron development through a separate mechanism, independent of its action on RGCs.

In summary, our work demonstrates that BDNF differentially influences presynaptic (axonal) and postsynaptic (dendritic) arbor structure in vivo. The observations that coordinated pre- and postsynaptic branching and synaptogenesis occurred under normal conditions or when retinotectal synaptic transmission was altered, but that alterations in BDNF levels elicited only delayed, corresponding changes in synapse innervation density suggest a novel mechanism by which BDNF influences the development of retinotectal connectivity in vivo (see Fig. 9). BDNF, through activation of TrkB receptors on RGCs, may induce the presynaptic RGC axons to spread their reach over a larger territory, thereby increasing the opportunity of the individual axon to come into contact with additional postsynaptic neurons. Simultaneously, BDNF may reinforce the emergent connectivity by stabilizing synapses and increasing synapse number with each and every postsynaptic partner. By modulating synapse number and strength in this manner, postsynaptic structure would remain unaffected, as the individual dendritic arbors would not need to grow to match the axon arbor. By contrast, a decline in TrkB signaling that results from the decreased availability of BDNF would negatively influence synaptic stability, reducing not only axon arbor extent but also synapse number and strength, ultimately influencing postsynaptic arbor shape. Thus, we propose that through its effects on presynaptic axons, BDNF can organize emergent retinotectal synaptic circuitry and modulate synaptic function and strength. By broadening the afferent synaptic input while simultaneously coordinating synapse formation and stabilization between pre- and postsynaptic neurons, BDNF can ultimately shape structural synaptic connectivity in the developing brain.

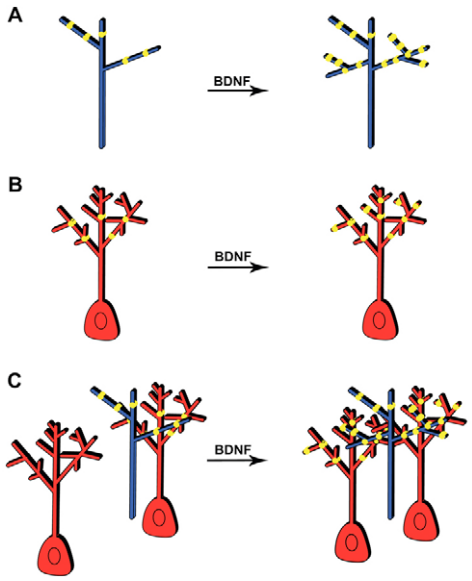

Fig. 9. The effects of BDNF during the development of retinotectal synaptic connectivity and their potential significance. (**A**) BDNF increases both arbor complexity and the density of presynaptic specializations in RGC axons. (**B**) BDNF increases the density of postsynaptic specializations on tectal neurons without influencing dendritic branch complexity. (**C**) BDNF, by increasing RGC axon arbor size and complexity, allows individual presynaptic RGC axon arbors to establish synaptic contacts with increased numbers of postsynaptic neurons. By modulating synapses directly, BDNF increases the density of synaptic innervation per tectal neuron. In a competitive scenario, the limiting amounts of BDNF would provide those presynaptic arbors directly exposed to BDNF a synaptic advantage and a greater opportunity to establish contacts with multiple postsynaptic partners.

We thank Dr D. Bredt for the gift of the PSD95-GFP construct, and Dr C. Ribak for expert advice and access to the electron microscope facility. We also thank Drs K. Cramer, R. Frostig and J. Campusano, and members of the laboratory for comments and critical reading of the manuscript. Supported by the NIH (EY11912).

References

Alsina, B., Vu, T. and Cohen-Cory, S. (2001). Visualizing synapse formation in arborizing optic axons in vivo: dynamics and modulation by BDNF. *Nat. Neurosci.* **4**, 1093-1101.

Baquet, Z. C., Gorski, J. A. and Jones, K. R. (2004). Early striatal dendrite deficits followed by neuron loss with advanced age in the absence of anterograde cortical brain-derived neurotrophic factor. *J. Neurosci.* **24**, 4250-4258.
Chen, Y. and Ghosh, A. (2005). Regulation of dendritic development by neuronal activity. *J. Neurobiol.* **64**, 4-10.
Cline, H. T. (1998). Topographic maps: developing roles of synaptic plasticity. *Curr. Biol.* **8**, R836-R839.
Cline, H. T. (2001). Dendritic arbor development and synaptogenesis. *Curr. Opin. Neurobiol.* **11**, 118-126.
Cohen-Cory, S. (2002). The developing synapse: construction and modulation of synaptic structures and circuits. *Science* **298**, 770-776.
Cohen-Cory, S. and Fraser, S. E. (1994). BDNF in the development of the visual system of Xenopus. *Neuron* **12**, 747-761.
Cohen-Cory, S. and Fraser, S. E. (1995). Effects of brain-derived neurotrophic factor on optic axon branching and remodelling in vivo. *Nature* **378**, 192-196.
Cohen-Cory, S., Escandon, E. and Fraser, S. E. (1996). The cellular patterns of BDNF and trkB expression suggest multiple roles for BDNF during Xenopus visual system development. *Dev. Biol.* **179**, 102-115.
Dailey, M. E. and Smith, S. J. (1996). The dynamics of dendritic structure in developing hippocampal slices. *J. Neurosci.* **16**, 2983-2994.
Deng, J. and Dunaevsky, A. (2005). Dynamics of dendritic spines and their afferent terminals: spines are more motile than presynaptic boutons. *Dev. Biol.* **277**, 366-377.
Du, J. L. and Poo, M. M. (2004). Rapid BDNF-induced retrograde synaptic modification in a developing retinotectal system. *Nature* **429**, 878-883.
Ebihara, T., Kawabata, I., Usui, S., Sobue, K. and Okabe, S. (2003). Synchronized formation and remodeling of postsynaptic densities: long-term visualization of hippocampal neurons expressing postsynaptic density proteins tagged with green fluorescent protein. *J. Neurosci.* **23**, 2170-2181.
Elmariah, S. B., Crumling, M. A., Parsons, T. D. and Balice-Gordon, R. J. (2004). Postsynaptic TrkB-mediated signaling modulates excitatory and inhibitory neurotransmitter receptor clustering at hippocampal synapses. *J. Neurosci.* **24**, 2380-2393.
Ethell, I. M. and Pasquale, E. B. (2005). Molecular mechanisms of dendritic spine development and remodeling. *Prog. Neurobiol.* **75**, 161-205.
Friedman, H. V., Bresler, T., Garner, C. C. and Ziv, N. E. (2000). Assembly of new individual excitatory synapses: time course and temporal order of synaptic molecule recruitment. *Neuron* **27**, 57-69.
Gonzalez, M., Ruggiero, F. P., Chang, Q., Shi, Y. J., Rich, M. M., Kraner, S. and Balice-Gordon, R. J. (1999). Disruption of Trkb-mediated signaling induces disassembly of postsynaptic receptor clusters at neuromuscular junctions. *Neuron* **24**, 567-583.
Horch, H. W. and Katz, L. C. (2002). BDNF release from single cells elicits local dendritic growth in nearby neurons. *Nat. Neurosci.* **5**, 1177-1184.
Hu, B., Nikolakopoulou, A. M. and Cohen-Cory, S. (2005). BDNF stabilizes synapses and maintains the structural complexity of optic axons in vivo. *Development* **132**, 4285-4298.
Ji, Y., Pang, P. T., Feng, L. and Lu, B. (2005). Cyclic AMP controls BDNF-induced TrkB phosphorylation and dendritic spine formation in mature hippocampal neurons. *Nat. Neurosci.* **8**, 164-172.
Jontes, J. D. and Smith, S. J. (2000). Filopodia, spines, and the generation of synaptic diversity. *Neuron* **27**, 11-14.
Kafitz, K. W., Rose, C. R., Thoenen, H. and Konnerth, A. (1999). Neurotrophin-evoked rapid excitation through TrkB receptors. *Nature* **401**, 918-921.
Konur, S. and Yuste, R. (2004). Imaging the motility of dendritic protrusions and axon terminals: roles in axon sampling and synaptic competition. *Mol. Cell Neurosci.* **27**, 427-440.
Kovalchuk, Y., Hanse, E., Kafitz, K. W. and Konnerth, A. (2002). Postsynaptic induction of BDNF-mediated long-term potentiation. *Science* **295**, 1729-1734.
Lom, B. and Cohen-Cory, S. (1999). Brain-derived neurotrophic factor differentially regulates retinal ganglion cell dendritic and axonal arborization in vivo. *J. Neurosci.* **19**, 9928-9938.
Lom, B., Cogen, J., Sanchez, A. L., Vu, T. and Cohen-Cory, S. (2002). Local and target-derived brain-derived neurotrophic factor exert opposing effects on the dendritic arborization of retinal ganglion cells in vivo. *J. Neurosci.* **22**, 7639-7649.
Luikart, B. W., Nef, S., Virmani, T., Lush, M. E., Liu, Y., Kavalali, E. T. and Parada, L. F. (2005). TrkB has a cell-autonomous role in the establishment of hippocampal Schaffer collateral synapses. *J. Neurosci.* **25**, 3774-3786.
Marrs, G. S., Green, S. H. and Dailey, M. E. (2001). Rapid formation and remodeling of postsynaptic densities in developing dendrites. *Nat. Neurosci.* **4**, 1006-1013.
McAllister, A. K. (2000). Cellular and molecular mechanisms of dendrite growth. *Cereb. Cortex* **10**, 963-973.
McAllister, A. K., Lo, D. C. and Katz, L. C. (1995). Neurotrophins regulate dendritic growth in developing visual cortex. *Neuron* **15**, 791-803.
McAllister, A. K., Katz, L. C. and Lo, D. C. (1997). Opposing roles for endogenous BDNF and NT-3 in regulating cortical dendritic growth. *Neuron* **18**, 767-778.
Niell, C. M., Meyer, M. P. and Smith, S. J. (2004). In vivo imaging of synapse formation on a growing dendritic arbor. *Nat. Neurosci.* **7**, 254-260.
Nieuwkoop, P. D. and Faber, J. (1956). *Normal Table of Xenopus laevis*. The Netherlands: Elsevier North Holland.
O'Rourke, N. A. and Fraser, S. E. (1990). Dynamic changes in optic fiber terminal arbors lead to retinotopic map formation: an in vivo confocal microscopic study. *Neuron* **5**, 159-171.
Okabe, S., Miwa, A. and Okado, H. (2001). Spine formation and correlated assembly of presynaptic and postsynaptic molecules. *J. Neurosci.* **21**, 6105-6114.
Rajan, I. and Cline, H. T. (1998). Glutamate receptor activity is required for normal development of tectal cell dendrites in vivo. *J. Neurosci.* **18**, 7836-7846.
Rajan, I., Witte, S. and Cline, H. T. (1999). NMDA receptor activity stabilizes presynaptic retinotectal axons and postsynaptic optic tectal cell dendrites in vivo. *J. Neurobiol.* **38**, 357-368.
Rico, B., Xu, B. and Reichardt, L. F. (2002). TrkB receptor signaling is required for establishment of GABAergic synapses in the cerebellum. *Nat. Neurosci.* **5**, 225-233.
Singh, K. K. and Miller, F. D. (2005). Activity regulates positive and negative neurotrophin-derived signals to determine axon competition. *Neuron* **45**, 837-845.
Trachtenberg, J. T., Chen, B. E., Knott, G. W., Feng, G., Sanes, J. R., Welker, E. and Svoboda, K. (2002). Long-term in vivo imaging of experience-dependent synaptic plasticity in adult cortex. *Nature* **420**, 788-794.
Umeda, T., Ebihara, T. and Okabe, S. (2005). Simultaneous observation of stably associated presynaptic varicosities and postsynaptic spines: morphological alterations of CA3-CA1 synapses in hippocampal slice cultures. *Mol. Cell Neurosci.* **28**, 264-274.
Vicario-Abejon, C., Owens, D., McKay, R. and Segal, M. (2002). Role of neurotrophins in central synapse formation and stabilization. *Nat. Rev. Neurosci.* **3**, 965-974.
von Bartheld, C. S., Wang, X. and Butowt, R. (2001). Anterograde axonal transport, transcytosis, and recycling of neurotrophic factors: the concept of trophic currencies in neural networks. *Mol. Neurobiol.* **24**, 1-28.
Waites, C. L., Craig, A. M. and Garner, C. C. (2005). Mechanisms of vertebrate synaptogenesis. *Annu. Rev. Neurosci.* **28**, 251-274.
Wirth, M. J., Brun, A., Grabert, J., Patz, S. and Wahle, P. (2003). Accelerated dendritic development of rat cortical pyramidal cells and interneurons after biolistic transfection with BDNF and NT4/5. *Development* **130**, 5827-5838.
Witte, S., Stier, H. and Cline, H. T. (1996). In vivo observations of timecourse and distribution of morphological dynamics in Xenopus retinotectal axon arbors. *J. Neurobiol.* **31**, 219-234.
Wu, G. Y. and Cline, H. T. (1998). Stabilization of dendritic arbor structure in vivo by CaMKII. *Science* **279**, 222-226.
Zhang, X. and Poo, M. M. (2002). Localized synaptic potentiation by BDNF requires local protein synthesis in the developing axon. *Neuron* **36**, 675-688.
Zweifel, L. S., Kuruvilla, R. and Ginty, D. D. (2005). Functions and mechanisms of retrograde neurotrophin signalling. *Nat. Rev. Neurosci.* **6**, 615-625.